CrossMark

Effective photocatalytic degradation of methylene blue by Cu$_2$O/MgAl layered double hydroxides

Yangmeihui Zhou[1] · Wenjihao Hu[1] · Jingang Yu[1] ·
Feipeng Jiao[1]

Abstract   A series of Cu$_2$O/MgAl layered double hydroxides (Cu$_2$O/LDHs) were first synthesized by an in situ method. X-ray diffraction analysis confirmed that Cu$_2$O/LDH calcined at 773 K calcination temperature (Cu$_2$O/CLDH-773) had a better crystal structure. N$_2$-adsorption/desorption isotherms and scanning electron microscopy images indicated that the resulting Cu$_2$O/CLDH-773 composite possesses high crystallinity, hierarchical structure as well as a large specific surface area. Energy dispersive X-ray spectroscopy and X-ray photoelectron spectroscopy were used to investigate the type and content of the elements in Cu$_2$O/CLDH-773. UV–Vis diffuse reflectance spectra confirmed that Cu$_2$O/CLDH-773 has an absorption band whose maximum falls in the visible region. The as-prepared Cu$_2$O/CLDH-773 displayed significant photocatalytic activity for the degradation of methylene blue (MB) under visible light irradiation. Factors that may affect the photodegradation of MB such as calcination temperature, LDHs content were studied. The stability of the photocatalysts was confirmed using reclaimed Cu$_2$O/CLDH-773 in four successive runs, and the results indicated that Cu$_2$O/CLDH-773 has a potential application in the field of photocatalysis. From the results of characterization and photodegradation, a possible mechanism for the photocatalytic dye degradation over Cu$_2$O/CLDH-773 was proposed.

Keywords   Layered double hydroxides · Cu$_2$O · Photocatalysis mechanism

✉ Feipeng Jiao
   jiaofp@csu.edu.cn

[1]   College of Chemistry and Chemical Engineering, Central South University, Changsha 410083, China

🖄 Springer

Introduction

Colored textile effluents contain persistent dyestuffs, many of which are very harmful, partially biodegradable, and do not undergo direct photolysis from sunlight [1]. Consequently, they accumulate in the environment. Therefore, effective treatment is necessary to dispose these reactive dyes. Photocatalytic oxidation is an advanced and highly effective technology for the degradation of a wide variety of pollutants in wastewater [2–4]. In recent years, it has attracted great attention because of the potential to use solar energy directly as a clean and renewable energy in photocatalytic process [5]. However, photocatalytic oxidation processes can be restricted by the low absorption of solar light, fast recombination of photogenerated electrons and holes, and low photocatalytic activity on the conventional crystal facets [6, 7]. In this regard, it is very significant to develop some novel stable visible-light-sensitive photocatalysts, which can degrade industrial pollutants efficiently.

Cuprous oxide (Cu_2O), one of the important materials in solar energy conversion and water splitting for hydrogen production under visible light irradiation, is a p-type semiconductor with the narrow direct band gap of 2.17 eV [8]. Recently, Cu_2O has also been used in the fields of photovoltaics, photocatalysis, gas sensors, Li ion battery research as well as optoelectronic applications [9]. However, because of the recombination between photogenerated electrons and holes, the difficulties in collecting for reuse, the easy aggregation or oxidation, the photocatalytic activity of pure Cu_2O is very low [10]. According to the reports, some methods have been developed in an attempt to enhance the photocatalytic activity of Cu_2O catalysts under visible light radiation, including construction of Cu_2O composites in core–shell nanostructures with noble metal, or combining with other semiconductors or co-adsorbents [11–14].

Layered double hydroxides (LDHs), known as anionic clays, have been further studied as catalysts and catalyst precursors during the past few decades [15, 16]. Because of the low cost, non-toxicity and easy preparation, LDHs are superior to other materials in environment remediation applications. Up to now, LDHs have found wide application in many scientific fields, such as catalysis, nanomedicine, separation and nanotechnology. Due to their large surface area, high anion exchange capacities and flexible interlayer space, LDHs also showed high uptake capacity [17]. The "memory effect" is another important property of LDHs. That is to say, the calcined LDH, which is composed of metal oxides, could be rehydrated again by contacting the solid with an anionic aqueous solution, and the hydrotalcite structure was then recovered by incorporating the solution anions. Therefore, LDHs can take up anion species from solution by three possible mechanisms: interlayer anion exchange, surface adsorption or reconstruction of calcined LDHs by the "memory effect" [18]. Furthermore, some typical literature articles report that LDHs may improve the efficiency of catalytic reactions through the enhancement of the pollutant adsorption and hydroxyl radical ($^{\cdot}OH$) production, and induce electron transfer [19, 20]. So, due to their fantastic properties, combining the high adsorptive capacity of LDHs with the high photocatalytic efficiency for the dye degradation, they may have a promising application in the removal of a variety of pollutants [21].

However, the photochemical applications of LDHs have been neglected and scarcely studied. Moreover, according to the extensive amount of publications, recent literature articles have seldom reported photocatalytic decomposition of an organic compound by using Cu_2O with catalyst supports of LDHs.

In this work, a series of Cu_2O/LDHs were first synthesized by a facile method. The structural, morphological, textural and semiconducting properties of as-synthesized solids were confirmed by XRD, SEM, EDX, N_2-adsorption/desorption, UV–Vis DRS and XPS methods. To evaluate their photocatalytic activities, methylene blue (MB) was selected as a model dye and degraded under visible light irradiation. Various factors such as calcination temperature and LDH content, which may affect the photodegradation efficiency, were investigated. The photocatalytic stability of LDHs was studied by multiple cycles using reclaimed catalysts. The possible mechanism underlying the enhanced photocatalytic activity and the electron transfer mechanism of Cu_2O/CLDH-773 were also discussed.

Experimental

Catalysts synthesis

MgAl-LDH

MgAl-LDH with Mg^{2+}/Al^{3+} ratio of 3.0 was prepared by the classical coprecipitation method [22]. Briefly, an aqueous solution containing $Mg(NO_3)_2 \cdot 6H_2O$ (0.075 mol) and $Al(NO_3)_3 \cdot 9H_2O$ (0.025 mol) was added to a vigorously stirred aqueous alkali solution of NaOH (1 M) and 0.075 mol of Na_2CO_3. The final value of the solution is 10. After heating at 353 K for 24 h, the obtained gel was washed thoroughly with deionized water until the pH was neutral. The resulting mixture was filtered, and the solid residue was collected and dried at 353 K overnight.

Cu_2O/LDH composites

To obtain the copper loaded materials, a wet impregnation method was used. A certain amount of $Cu(NO_3)_2 \cdot 3H_2O$ was dissolved in 80 mL distilled water, which was mixed with LDHs to form different Cu/LDH weight ratios: 1:2, 1:1 and 1.5:1. After stirring, the mixtures were centrifuged and washed by deionized water for several times to remove free Cu^{2+} ions. The mixture was added into 80 mL 1 M NaOH solution to form a suspension, which was then heated to 333 K in water bath under stirring. Then 500 mg glucose was added into the suspension until the color turned to brick red. After an additional 15 min of stirring, the product was centrifuged, washed with deionized water and ethanol, dried under vacuum for 4 h at 333 K. The Cu_2O/LDH (Cu/LDH = 1:1) samples were calcined under N_2 atmosphere at 673, 773 and 873 K with a constant heating rate of 5 K/min for 4 h. The obtained composites at different calcination temperatures were denoted as Cu_2O/CLDH-673, Cu_2O/CLDH-773, Cu_2O/CLDH-873. A series of Cu_2O/LDH

with different Cu/LDH ratios (1:2, 1:1 and 1.5:1) were also calcined under N_2 atmosphere at 773 K for 4 h.

The CuO/CLDH-773 nanoparticle was also synthesized by the same precipitation method of Cu_2O/CLDH-773 without glucose. After calcination, all the samples were cooled to room temperature slowly and stored in light proof vials prior to adsorption and photocatalytic tests. In order to establish the adsorption–desorption equilibrium between the dye and the catalyst surface, the reaction mixtures, which contained 400 mg catalyst and 400 mL MB, were stirred for 1 h under dark. After stirring, the Cu_2O/CLDH-773 nanoparticle was extracted and centrifuged, the obtained particle was denoted as Cu_2O/RLDH-773.

Photocatalytic tests

Continuous illumination was given by the photochemical reaction apparatus (BL-GHX-I) equipped with 300 W xenon lamp ($\lambda > 420$ nm) as a source of visible light. The photocatalytic activity of the prepared composites was evaluated by MB photodegradation tests. MB was selected because of its strong adsorption to metal oxide surfaces, well defined optical absorption and good resistance to light degradation [23]. 400 mg catalyst was suspended in 400 mL aqueous solution of MB (10 mg/L) at 298 K, pH 6.8 and the mixture was given a light with a wavelength of 420 nm. At given time intervals, 5 mL of different samples were extracted, centrifuged and filtered, respectively. The filtrates were analyzed using a UV–Vis spectrophotometer (UV-9600) by measuring the absorbance at a wavelength of $\lambda_{max} = 664$ nm. The blank reaction was carried out using a same sample procedure without adding catalyst. The degradation percentage of MB was calculated by $(1 - C/C_0) \times 100$ %, where C is MB concentration in aqueous solution at time t (mg/L), C_0 is initial MB concentration (mg/L) at t = 0.

Characterization

The X-ray diffraction (XRD) patterns were recorded on a powder X-ray diffractometer (Bruker D8) using Cu K_α ($\lambda = 1.5406$ Å) radiation at a voltage of 40 kV and a current of 40 mA. The samples were scanned in steps of 0.04° (2θ) in the range of 5–70° with a count time of 4 s per step. The UV–Vis diffuse reflectance spectra (UV–Vis DRS) of the samples were recorded in the range of 200–700 nm on a Schimadzu 2401 UV–Vis spectrophotometer with an integrating diffuse reflective sphere and $BaSO_4$ as reference. The Brunauer–Emmett–Teller (BET) surface areas of the samples were calculated from N_2 adsorption–desorption experiments determined at 77 K using a Quantachrome Autosorb-1 system. Scanning electron microscopy (SEM) investigation was carried out for all samples using a JSM-6360LV microscope operating at an acceleration voltage of 25 keV. Energy dispersive X-ray spectroscopy (EDX) was used to investigate the chemical composition of the samples. X-ray photoelectron spectroscopy (XPS) analysis was performed on a K-Alpha 1063 system, using monochromatic Al K_α radiation (1253.6 eV) operating at 75 W, with a spot area of 400 mm. All binding energies (BE) were referenced to the C 1 s peak at 284.6 eV. The experimental errors were within ±0.1 eV.

Results and discussion

Material characterization

XRD

XRD was used to identify and determine the phase structure of the samples. Fig. 1a shows the XRD patterns of the as-prepared MgAl-LDH, Cu_2O, Cu_2O/CLDH-773 and Cu_2O/RLDH-773. From the XRD peaks of MgAl-LDH, the characteristic reflections of a well-ordered lay structure (003) and (006) can be found (JCPDF. 41-1428). In the XRD pattern of the as-prepared pure Cu_2O, there were six clear peaks with 2θ values of 30.14°, 37.00°, 42.90°, 62.02°, 74.2° and 78.08°,
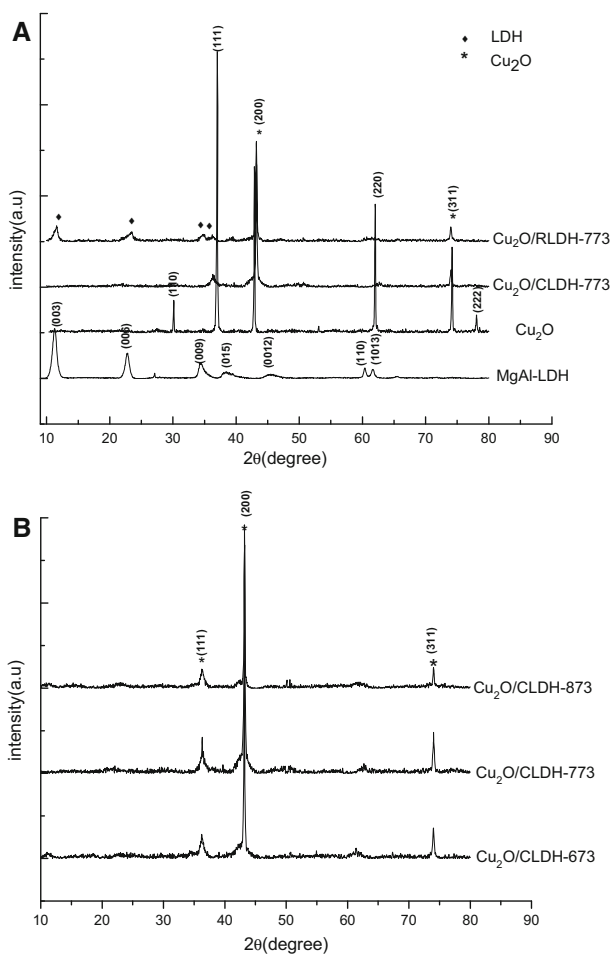
Fig. 1 **a** XRD patterns of MgAl-LDH, Cu_2O, Cu_2O/CLDH-773 and Cu_2O/RLDH-773; **b** XRD patterns of Cu_2O/RLDH-673, Cu_2O/RLDH-773 and Cu_2O/RLDH-873

corresponding to the crystal planes of (110), (111), (200), (220), (311) and (222) of crystalline Cu_2O (JCPDF. 65-3288). Fig. 1a indicates that the characteristic reflections (003) and (006) of the Cu_2O/CLDH-773 disappeared after calcination. However, after the adsorption–desorption process, the re-appearance of (003) and (006) reflections of Cu_2O/RLDH-773 confirm the "memory effect" of the LDH precursor. That is to say, the layer structure was recovered after stirred 1 h in the dark. This phenomenon may be due to the dissolved CO_2, which could generate to CO_3^{2-} in the solution.

The effects of calcination temperature on the structural properties and the crystallite sizes have been studied by XRD (Fig. 1b). The XRD analysis of the calcined Cu_2O/LDHs at different calcination temperatures shows that all the products are well crystallized. It can be seen that all samples show exceptionally strong (200) reflection peaks and extremely weak (111) reflection peaks at calcination temperatures 673, 773, 873 K. According to the XRD results, it can be deduced that the Cu_2O phase transforms from (111) to (200) when the calcination temperature reached 673 K or exceeded 673 K. In addition, the observed diffraction peaks of Cu_2O/CLDH-773 are slightly more intense, indicating that a better crystal structure was formed at a calcination temperature of 773 K.

SEM and EDX

The morphological and microstructural details of the as-prepared particles were investigated by SEM. From the magnified image in Fig. 2a, it can be seen clearly that the loaded Cu_2O particles are uniformly embedded into the entire MgAl-LDH frame, including the surface, internal and external walls of the MgAl-LDH. Fig. 2a shows that the surface of Cu_2O/CLDH-773 was rough and porous because Cu_2O particles were wrapped in MgAl-LDH during the growth. Additionally, the rough surface of MgAl-LDH can prevent Cu_2O from aggregation, leading to a formation of discrete Cu_2O particles. It can be seen from Fig. 2b that the image of hydrangea-like particles reveals that the LDH structure has been regenerated after adsorption–desorption process, which is in good agreement with the XRD results. Moreover, it is interesting to observe that the regeneration of Mg/Al-LDH would present platelet-shaped particles with average size of 500–1000 nm, which can offer more active adsorption sites and photocatalytic reaction sites. EDX analysis confirmed that Cu_2O/CLDH-773 nanosheet is composed of Mg, Al, O and Cu elements (Fig. 2c).

XPS

XPS analysis can be used to confirm the chemical valence of Cu element. According to previous reports, for the CuO_X (Cu_2O, CuO or their mixture), the typical XPS peaks of Cu^+ and Cu^{2+} in the Cu $2p_{3/2}$ region appear around 932.6 and 933.7 eV, respectively [24]. The high resolution XPS of Cu in the 2p region for Cu_2O/CLDH-773 is shown in Fig. 3a. The sharp peak without any satellite located at 932.68 eV is corresponding to Cu^+, which can be attributed to Cu_2O on the surface of calcined MgAl-LDH nanosheet (CLDH). Furthermore, no peaks can be found around 933.7 eV, indicating that Cu species on the surface of CLDH nanosheet only exist
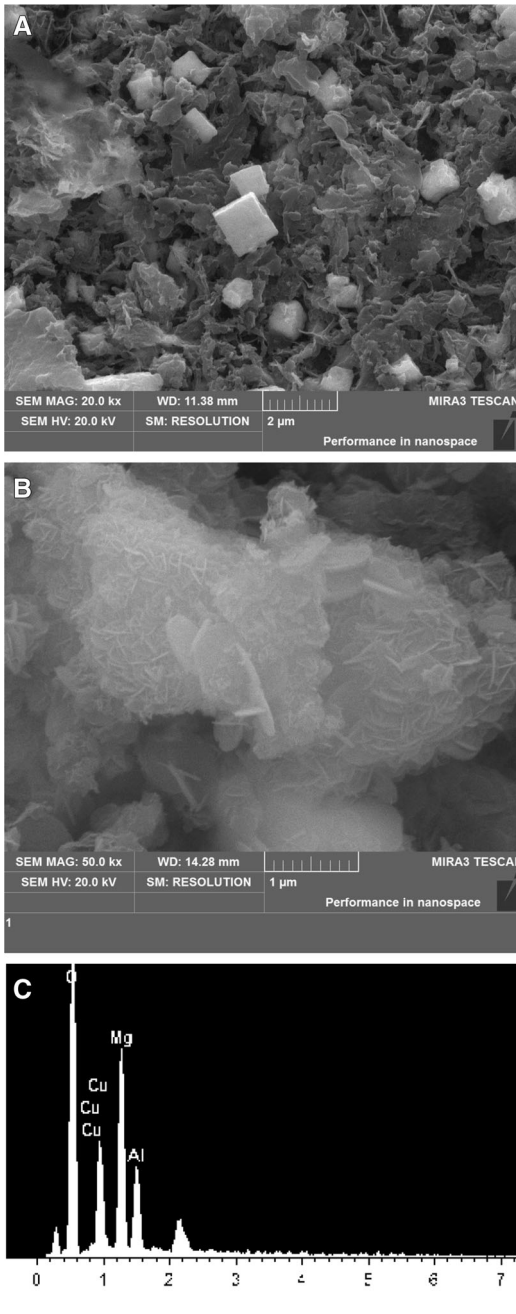
Fig. 2 **a** SEM image of $Cu_2O/CLDH$-773; **b** SEM image of $Cu_2O/RLDH$-773; **c** EDX spectrum from $Cu_2O/CLDH$-773
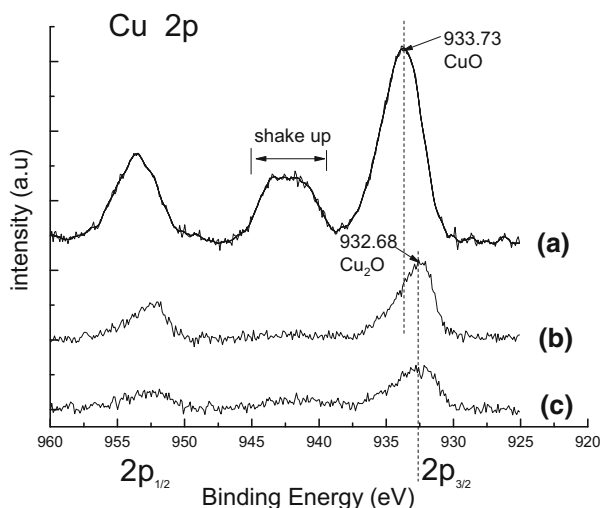
Fig. 3 High-resolution XPS spectra of Cu 2p region for fresh Cu_2O/CLDH-773 (**a**), CuO/CLDH-773 (**b**), and used Cu_2O/CLDH-773 after four cycles

as +1 valence state. In order to verify the identification of Cu_2O and CuO, XPS spectra of CuO/CLDH-773 was tested (Fig. 3b), and the presence of a strong peak at 933.73 eV is related to Cu^{2+} $2p_{3/2}$. The strong shake-up satellite peak from 941 to 945 eV is related to the trace amounts of CuO with a d^9 electron configuration in ground state [25]. Based on SEM and XPS results, it can be deduced that discrete Cu_2O nanoparticles could be formed on the surface of CLDH nanosheet.

To evaluate the chemical stability of Cu_2O during photocatalysis, we detect the XPS spectrum of Cu_2O/CLDH-773 after four photocatalytic cycles. From Fig. 3c, it can be seen that the peak at 932.6 eV corresponding to Cu^+ in Cu $2p_{3/2}$ region is always there, indicating that the Cu_2O nanoparticles were very stable during the photocatalytic process. Based on the survey spectrum of overall samples, it can be concluded that copper element exists as +1 valence state on the surface of CLDHs. Moreover, Cu_2O nanoparticles are stable enough during the photocatalytic process.

UV–Vis

To gather further insights into the absorption of UV and visible light by the as-prepared catalysts, the samples were analyzed by UV–Vis diffuse reflectance spectroscopy. As shown in Fig. 4, MgAl-LDH calcined at 773 K (CLDH-773) possesses a clear absorption edge at about 430 nm, indicating that the CLDH-773 absorbs in the UV region mostly. In contrast, Cu_2O displays obvious absorption up to 660 nm. As for Cu_2O/CLDH-773, a broad visible light absorption at 400–800 nm can be seen in all Cu_2O/CLDH-773, indicating their promising applications for the utilization of solar energy. The result can be explained that the anionic clays LDHs, which have abundant OH groups, could promote electron transfer, so Cu_2O/CLDH-773 has a red-shift in light absorption compared to pure Cu_2O [26].

BET surface area and pore size distribution

Fig. 5 shows BET surface area and pore size distribution for the $Cu_2O/CLDH-773$. As shown in this figure, the sample had the isotherms of type IV with the hysteresis loop of type H3, which characterizes mesoporous solids, according to the IUPAC classification. The hysteresis loop is of type H3, which is commonly attributed to slit-shaped pores generated by the aggregation of plate-like particles [27]. The
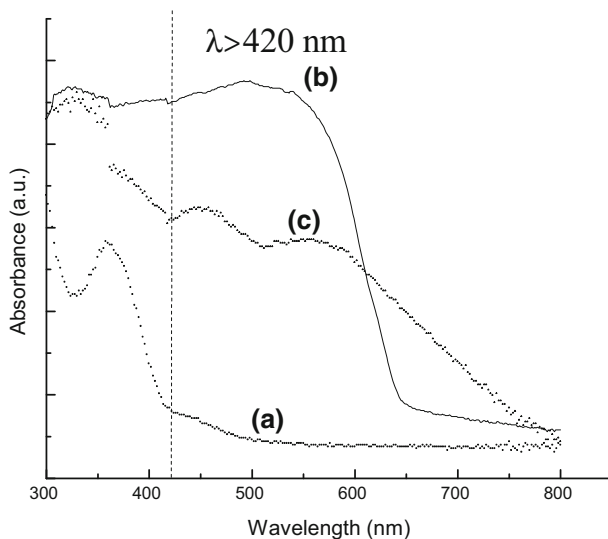

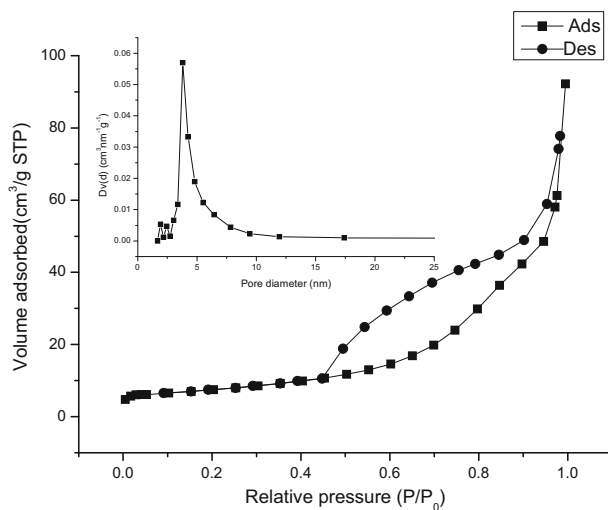**Fig. 4** UV–Vis DRS of CLDH-773 (**a**), Cu_2O (**b**), and $Cu_2O/CLDH-773$ (**c**)

Fig. 5 N_2 adsorption–desorption isotherm and corresponding pore size distribution of $Cu_2O/CLDH-773$

isotherms showed high absorption at high relative pressure $P/P_0 = 0.990$. In calcined LDHs, the smallest pores are considered as intraparticle pores formed during calcination, due to a "cratering" process [28]. With the disorderly collapse and stacking of plate-like particles, the larger mesopores and the macropores are formed during calcination. Therefore, interparticle porosity depends on crystallinity and particle size of original LDHs [28]. According to the XRD results, Cu_2O/CLDH-773 had a better crystal structure with respect to other samples calcined at 873 and 673 K, so after the collapse of particles during the calcination process, the stacking arrangement was better ordered and more closely aggregated, smaller and more uniform interparticle pores were obtained as a result.

Photocatalytic activity for the degradation of dye

Effect of various catalyst

The photocatalytic behaviors of MgAl-LDH, Cu_2O/LDH (Cu/LDH = 1:1), CLDH-773, Cu_2O/CLDH-773 samples were measured by the degradation of MB under visible light irradiation, and the results are shown in Fig. 6. From Fig. 6a, the degradation of MB in the absence of catalyst is only about 13.9 %, demonstrating that the self-degradation of MB is rather slow. A similar phenomenon has been observed in the recent work by Jurng et al. [23], which was ascribed to the photoexcited self-degradation of MB. Besides, the adsorption behavior of MB on the Cu_2O/CLDH-773 was studied in the dark, indicating that the period of 1 h is long enough to reach the equilibrium before the photodegradation. Moreover, Fig. 6b shows that under the same reaction conditions, the MgAl-LDH and CLDH-773 samples exhibit a low visible light photocatalytic activity for aqueous MB degradation, and their photodegradation efficiencies are about 31.9 and 42.2 %. The low photocatalytic activities can be ascribed to the small absorption of visible light by LDHs. However, the Cu_2O/LDH (Cu/LDH = 1:1) sample shows a higher visible light photocatalytic activity (51.8 %). The results indicate that the Cu_2O plays an important role in the photocatalytic activity. Compared with the pure Cu_2O, Cu_2O/CLDH-773 has better photodegradation efficiency achieved 86.2 %. The high photoactivity of Cu_2O/CLDH-773 can be explained that the calcined LDHs could offer more active adsorption sites and photocatalytic reaction centers, which is corresponding to the SEM and BET results.

Effect of different ratio

Fig. 7 shows the results of the influence of the Cu/LDH molar ratio on the degradation of MB at the same conditions. As shown in Fig. 7, it is obvious that the degradation amounts of MB increased with the increase of the weight ratio of Cu/LDH and reaches maximum 86.2 % at an optimal weight ratio Cu/LDH of 1.0. With further increase in the weight ratio of Cu/LDH up to 1.5, there has been a decrease in the degradation of MB. When the weight ratio is lower than its optimal amount, the low photocatalytic degradation 63.2 % can be due to the agglomeration of the Mg/Al-LDH particles, which is not conducive to the reaction between Cu_2O

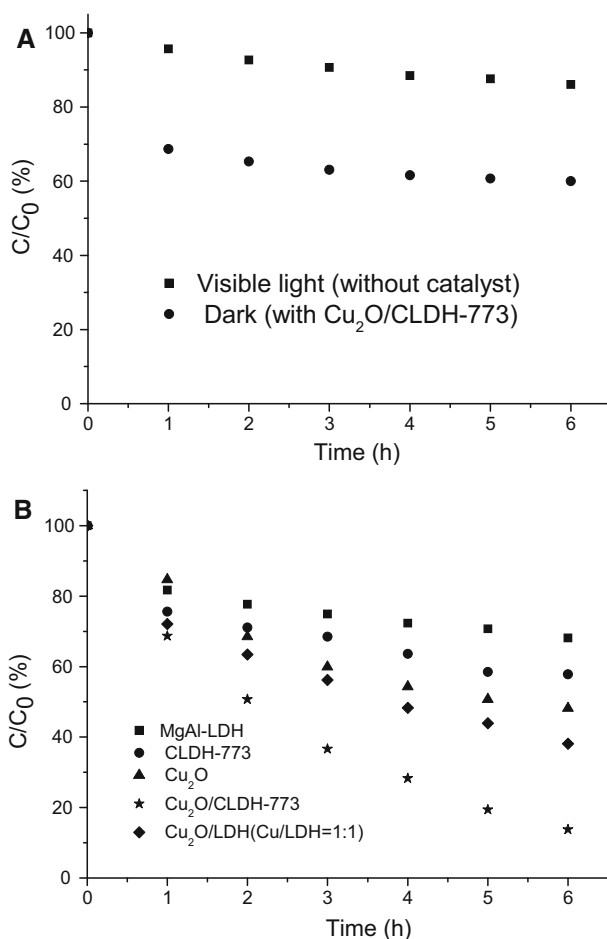**Fig. 6** **a** The adsorption experiment in dark using $Cu_2O/CLDH$-773 and MB degradation experiment without catalyst under visible light irradiation (MB = 10 mg/L, pH = 6.8, T = 298 K); **b** comparative studies of the photocatalytic activity of the different samples under visible light irradiation (MB = 10 mg/L, pH = 6.8, T = 298 K)

and MB. In addition, the aggregation of the Mg/Al-LDH can lead to a decrease in the total surface area. The insufficient Mg/Al-LDH particles may decrease the number of active adsorption sites and photocatalytic reaction sites. Clearly, there is an optimal weight ratio Cu/LDH of 1.0 to exhibit the highest photocatalysis activity. Consequently, an optimized weight ratio of Cu/LDH 1.0 is used for the other experiments in this study.

Effect of various calcination temperatures

Calcination may bring about a thermal decomposition, phase transition, or removal of a volatile fraction. Taking into the important role of calcination temperature in
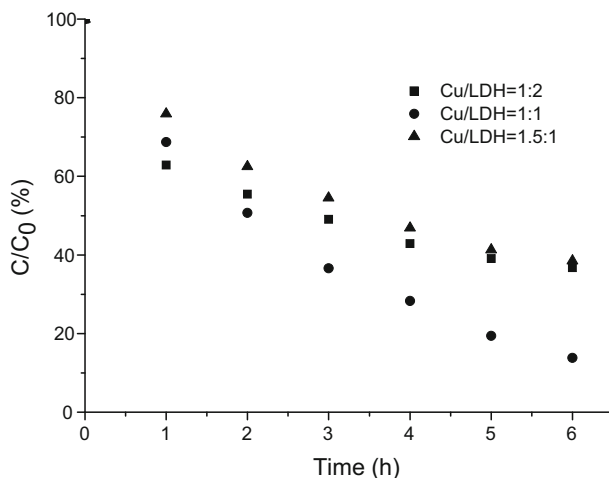
Fig. 7 Effect of Cu/LDH molar ratio on the degradation of MB (10 mg/L) under visible light irradiation (pH = 6.8, T = 298 K)
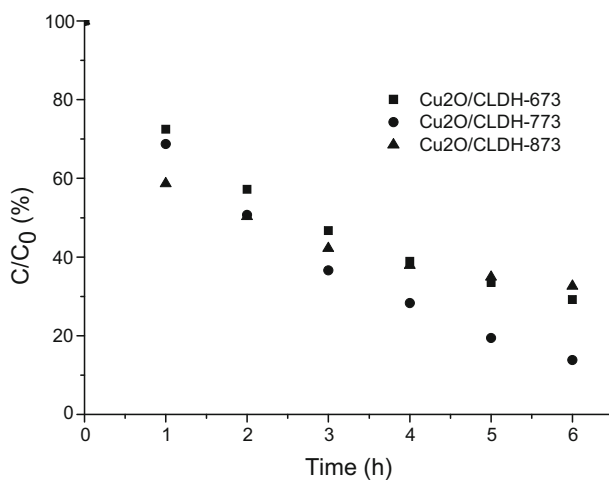

Fig. 8 Effect of Cu_2O/CLDH at different calcination temperatures for 4 h on MB (10 mg/L) degradation under visible light irradiation (pH = 6.8, T = 298 K)

the structural properties of catalysts, Cu_2O/LDHs were calcined at various temperatures (673–873 K). The results of the effect of different calcination temperatures on the photocatalytic activity are shown in Fig. 8. It is found that the Cu_2O/LDHs at calcination temperatures 673, 773 and 873 K display high photocatalytic activity under visible-light irradiation and the degradation of MB are 70.8, 86.2 and 67.3 %, in order. The photocatalyst calcined at 773 K exhibits the highest photocatalytic activity under visible light irradiation than the other calcined
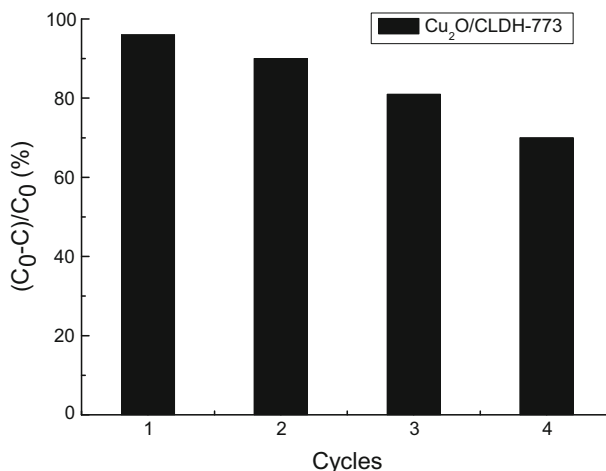
Fig. 9 Photocatalytic cycles of $Cu_2O/CLDH-773$ under visible light irradiation (MB = 10 mg/L, pH = 6.8, T = 298 K)

catalysts, which is mainly due to the highest crystallinity of Cu_2O, as shown by the XRD patterns (Fig. 1b).
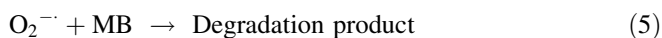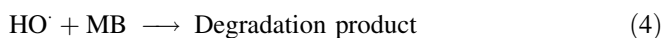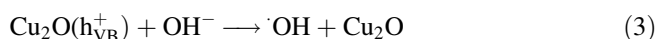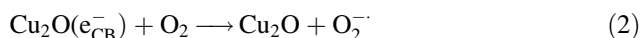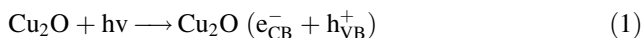
Stability of photocatalys

The regeneration of catalyst is one of the key aspects to make catalysis technology for practical applications. To test the stability of the photocatalysts, $Cu_2O/CLDH$-773 as a representative photocatalyst is used for 4 times of photodegradation of MB. The catalysts were recovered by filtration, washed with ethanol, and then dried overnight at 353 K for 24 h under vacuum. As indicated in Fig. 9, the photocatalytic activity is still higher than 80 % for reused $Cu_2O/CLDH$-773. These results illustrate that the catalyst has higher stability and it can be reusable. The photocatalytic activity percentage decreases if we reuse the catalyst for a third and fourth time. Furthermore, from the above results, it is clear that the catalyst is not stable more than two runs. The reason for such a decrease in photocatalytic activity may be the decrease of surface active sites caused by adsorption of dye molecules and the catalyst loss during the process of washing.

Electron transfer mechanism

It is well known that the light absorption capability of photocatalyst and separation of excited electron–hole pair play important roles during the whole photoactivity process. From all experimental results mentioned above, a possible mechanism for the photodegradation of MB over $Cu_2O/CLDH$-773 composite catalyst has been proposed. The LDH effect on the activity of Cu_2O can be explained in terms of its action as dispersing agents, adsorbent materials and OH groups providers, which increase adsorption and can react with the excited holes to form hydroxyl radicals

(˙OH). Indeed, as shown in Figs. 6 and 7, for mixed 1:1 samples, the activities were higher than that of pure Cu_2O. Furthermore, the introduction of LDHs can improve the pollutant adsorption and ˙OH production from the results of BET and SEM. According to the results of the electron microscopy and the BET analysis, the surface of Cu_2O/CLDH-773 was rough and porous, which could increase the specific surface area of the composite to improve its adsorption ability. Additionally, the narrow band gap of Cu_2O makes it capable of absorbing visible light to generate photoelectrons and holes at the conduction and valence bands, respectively. However, when Cu_2O particles loaded on LDHs, more photo-generated electrons could be captured by adsorbed O_2 on the surface of Cu_2O/CLDH-773 to yield O_2^{-}˙, which may restrain the recombination between photo-generated electrons and holes to improve the photocatalytic activity of Cu_2O/CLDH-773. The holes left in the valence band of Cu_2O can react with the OH groups derived from LDHs and form ˙OH. Here, photocatalysis takes place by the well-known mechanism of visible-light-driven electron excitation from the valence band to the conduction band, the formation of oxidative intermediate species O_2^{-}˙ and ˙OH in turn degrade the MB [29].

Based on the above discussion, we think that the combining of LDHs and Cu_2O via in situ preparation process greatly improves the adsorption ability of the composite and promotes the separation of photo-generated electrons–holes pair, accordingly, a higher photocatalytic activity is achieved.

$$Cu_2O + h\nu \longrightarrow Cu_2O\ (e_{CB}^{-} + h_{VB}^{+}) \tag{1}$$

$$Cu_2O(e_{CB}^{-}) + O_2 \longrightarrow Cu_2O + O_2^{-\cdot} \tag{2}$$

$$Cu_2O(h_{VB}^{+}) + OH^{-} \longrightarrow {}^{\cdot}OH + Cu_2O \tag{3}$$

$$HO^{\cdot} + MB \longrightarrow Degradation\ product \tag{4}$$

$$O_2^{-\cdot} + MB \rightarrow Degradation\ product \tag{5}$$

Conclusion

A series of Cu_2O/LDHs were first synthesizded by an in situ method. The as-prepared Cu_2O/CLDH-773 showed higher photocatalytic activity for the degradation of MB compared to laboratory-made MgAl-LDH and Cu_2O under solar light irradiation. Calcined LDHs are optically transparent in the visible region according to UV–Vis DRS results. SEM and BET investigations confirmed that the introduction of LDHs could increase the specific surface area and active sites, restrain the recombination among photogenerated electrons and holes, and prevent Cu_2O from aggregation. It is found that the Cu_2O/CLDH-773 displays high photocatalytic activity under visible light irradiation and the degradation of MB is 86.2 %. In addition, the introduction of an optimum amount of LDHs (Cu/LDH = 1:1) could enhance the photocatalytic properties. A possible mechanism of photocatalytic dye degradation over Cu_2O/

CLDH-773 was proposed according to the experimental results. Cu_2O/LDHs possess the advantages of facile preparation process, stable, low cost and environment friendly. Moreover, the catalysts can be reused, the degradation ratio is still higher than 80 % after two cycles. Hence, the application of Cu_2O/LDHs for the photodegradation of a wide variety of aqueous contaminants is expected.

References

1. Liu X, Zhao X, Zhu Y, Zhang F (2013) Experimental and theoretical investigation into the elimination of organic pollutants from solution by layered double hydroxides. Appl Catal B 140–141:241–248
2. Mahmoodi NM (2011) Photocatalytic ozonation of dyes using copper ferrite nanoparticle prepared by co-precipitation method. Desalination 279:332–337
3. Huo C, Yang H (2013) Preparation and enhanced photocatalytic activity of Pd-CuO/palygorskite nanocomposites. Appl Clay Sci 74:87–94
4. Huang Z, Wu P, Lu Y, Wang X, Zhu N, Dang Z (2013) Enhancement of photocatalytic degradation of dimethyl phthalate with nano-TiO_2 immobilized onto hydrophobic layered double hydroxides: a mechanism study. J Hazard Mater 246:70–78
5. Chong MN, Jin B, Chow ChWK, Saint C (2010) Recent developments in photocatalytic water treatment technology: a review. Water Res 44:2997–3027
6. Lu R, Xu X, Chang J, Zhu Y, Xu S, Zhang F (2012) Improvement of photocatalytic activity of TiO_2 nanoparticles on selectively reconstructed layered double hydroxide. Appl Catal B 111–112:389–396
7. Abdulkarem AM, Aref AA, Abdulhabeeb A, Li YF, Yu Y (2013) Synthesis of Bi_2O_3/Cu_2O nanoflowers by hydrothermal method and its photocatalytic activity enhancement under simulated sunlight. J Alloy Compd 560:132–141
8. Heng B, Xiao T, Hu X, Yuan M, Tao W, Huang W, Tang Y (2011) Catalytic activity of Cu_2O microparticles with different morphologies in the thermal decomposition of ammonium perchlorate. Thermochim Acta 524:135–139
9. Khanderi J, Contiu C, Engstler J, Hoffmann RC, Schneider JJ, Drochner A, Vogel H (2011) Binary [Cu_2O/MWCNT] and ternary [Cu_2O/ZnO/MWCNT] nanocomposites: formation, characterization and catalytic performance in partial ethanol oxidation. Nanoscale 3:1102–1112
10. Cao C, Xiao L, Liu L, Zhu H, Chen C, Gao L (2013) Visible-light photocatalytic decolorization of reactive brilliant red X-3B on Cu_2O/crosslinked-chitosan nanocomposites prepared via one step process. Appl Surf Sci 271:105–112
11. Wang W, Huang X, Wu S, Zhou Y, Wang L, Shi H, Liang Y, Zou B (2013) Preparation of p–n junction Cu_2O/$BiVO_4$ heterogeneous nanostructures with enhanced visible-light photocatalytic activity. Appl Catal B 134–135:293–301
12. Zhang Z, Che H, Wang Y, Gao J, Ping Y, Zhong Z, Su F (2012) Template-free synthesis of Cu@Cu_2O core–shell microspheres and their application as copper-based catalysts for dimethyldichlorosilane synthesis. Chem Eng J 211–212:421–431
13. Yang R, Ma F, Tao T, Tang D, Ren Y, Chen Z, Zhang X, Xu M (2013) Zn^{2+}-assisted synthesis of concave Cu_2O crystals and enhanced photocatalytic properties. Catal Commun 42:109–112
14. Tian Y, Chang B, Fu J, Zhou B, Liu J, Xi F, Dong X (2014) Graphitic carbon nitride/Cu_2O heterojunctions: preparation, characterization, and enhanced photocatalytic activity under visible light. J Solid State Chem 212:1–6
15. Silva CG, Bouizi Y, Fornés V, García H (2009) Layered double hydroxides as highly efficient photocatalysts for visible light oxygen generation from water. J Am Chem Soc 131:13833–13839
16. Dvininov E, Ignat M, Barvinschi P, Smithers MA, Popovici E (2010) New SnO_2/MgAl-layered double hydroxide composites as photocatalysts for cationic dyes bleaching. J Hazard Mater 177:150–158

17. Mantilla A, Tzompantzi F, Fernandez JL, Diaz Gongora JAI, Gomez R (2010) Photodegradation of phenol and cresol in aqueous medium by using Zn/Al + Fe mixed oxides obtained from layered double hydroxides materials. Catal Today 150:353–357
18. Carja G, Dartu L, Okada K, Fortunato E (2013) Nanoparticles of copper oxide on layered double hydroxides and the derived solid solutions as wide spectrum active nano-photocatalysts. Chem Eng J 222:60–66
19. Zhang FZ, Xiang X, Li F, Duan X (2008) Layered double hydroxides as catalytic materials: recent development. Catal Surv Asia 12:253–265
20. Parida K, Mohapatra L (2012) Recent progress in the development of carbonate-intercalated Zn/Cr LDH as a novel photocatalyst for hydrogen evolution aimed at the utilization of solar light. Dalton T 41:1173–1178
21. Tian L, Zhao Y, He S, Wei M, Duan X (2012) Immobilized Cu–Cr layered double hydroxide films with visible-light responsive photocatalysis for organic pollutants. Chem Eng J 184:261–267
22. Du LC, Qu BJ, Zhang M (2007) Thermal properties and combustion characterization of nylon 6/MgAl-LDH nanocomposites via organic modification and melt intercalation. Polym Degrad Stab 92:497–502
23. Le HA, Linh LT, Chin S, Jurng J (2012) Photocatalytic degradation of methylene blue by a combination of TiO_2-anatase and coconut shell activated carbon. Powder Technol 225:167–175
24. Liu L, Gu X, Sun C, Li H, Deng Y, Gao F, Dong L (2012) In situ loading of ultra-small Cu2O particles on TiO_2 nanosheets to enhance the visible-light photoactivity. Nanoscale 4:6351–6359
25. Pearce CI, Pattrick RAD, Vaughan DJ, Henderson CMB, van der Laan G (2006) Copper oxidation state in chalcopyrite: Mixed Cu d^9 and d^{10} characteristics. Geochim Cosmochim Acta 70:4635–4642
26. Paredes SP, Valenzuela M, Fetter G, Flores SO (2011) TiO_2/MgAl layered double hydroxides mechanical mixtures as efficient photocatalysts in phenol degradation. J Phys Chem Solids 72:914–919
27. Valente JS, Tzompantzi F, Prince J, Cortez JGH, Gomez R (2009) Adsorption and photocatalytic degradation of phenol and 2,4 dichlorophenoxiacetic acid by Mg–Zn–Al layered double hydroxides. Appl Catal B 90:330–338
28. Valente JS, Tzompantzi F, Prince J (2011) Highly efficient photocatalytic elimination of phenol and chlorinated phenols by CeO_2/MgAl layered double hydroxides. Appl Catal B 102:276–285
29. Burrows HD, Ernestova LS, Kemp TJ, Skurlatov YI, Purmal AP, Yermakov AN (1998) Kinetics and mechanism of photodegradation of chlorophenols. Prog React Kinet 23:145–207